Invariant-Based Inverse Engineering of Crane Control Parameters

S. González-Resines,[1] D. Guéry-Odelin,[2] A. Tobalina,[1] I. Lizuain,[3] E. Torrontegui,[4] and J. G. Muga[1,*]

[1]*Departamento de Química Física, UPV/EHU, Apartado 644, 48080 Bilbao, Spain*

[2]*Laboratoire de Collisions Agrégats Réactivité, CNRS UMR 5589, IRSAMC, Université de Toulouse (UPS), 118 Route de Narbonne, 31062 Toulouse CEDEX 4, France*

[3]*Department of Applied Mathematics, University of the Basque Country UPV/EHU, Plaza Europa 1, 20018 Donostia-San Sebastian, Spain*

[4]*Instituto de Física Fundamental IFF-CSIC, Calle Serrano 113b, 28006 Madrid, Spain*

(Received 19 May 2017; revised manuscript received 20 September 2017; published 6 November 2017)

By applying invariant-based inverse engineering in the small-oscillation regime, we design the time dependence of the control parameters of an overhead crane (trolley displacement and rope length) to transport a load between two positions at different heights with minimal final-energy excitation for a microcanonical ensemble of initial conditions. The analogy between ion transport in multisegmented traps or neutral-atom transport in moving optical lattices and load manipulation by cranes opens a route for a useful transfer of techniques among very different fields.

DOI: 10.1103/PhysRevApplied.8.054008

I. INTRODUCTION

The similarities between the mathematical descriptions of different systems have been repeatedly applied in the history of physics, and they continue to play a heuristic and fruitful role. The entire field of quantum simulations [1–4] and the design of optical waveguide devices based on its analogy with quantum-mechanical discrete systems [5–9] are current examples. The usefulness of analogies was addressed by Maxwell [10], who wrote, "In many cases the relations of the phenomena in two different physical questions have a certain similarity which enables us, when we have solved one of these questions, to make use of our solution in answering the other." He also warned about the dangers of pushing the analogy beyond certain limits, and the need for a "judicious use" [10].

Our first aim in this work is to detail a connection between two very different systems so as to, following Maxwell's advice, judiciously take advantage of the similarities for mutual benefit by transferring knowledge and control techniques. Specifically, the systems in question are (i) ultracold ions or neutral atoms in effectively one-dimensional traps with time-dependent controllable parameters, as used in recent advances towards scalable quantum-information processing [11,12], and (ii) payloads moved by industrial or construction cranes [13]. In spite of the different orders of magnitude in the masses and sizes involved, both systems are described in the harmonic limit of small oscillations by similar mass-independent equations. They require manipulation approaches to achieve the same goals, namely, to transfer a mass quickly, safely, and without final excitation to a preselected location. The need to implement robust protocols with respect to on-route perturbations or initial-state dispersion is also common. Quantumness may play a role beyond the harmonic domain, and it precludes a naive direct translation from the macroscopic to the microscopic world of control techniques based on feedback from measurements performed on route. However, in the harmonic regime, the equations used for inverse engineering the control parameters in open-loop approaches (without feedback control) of a crane can be identical to those used to determine the motion of traps that drive microscopic particles. These approaches may as well have common elements for quantum and classical systems beyond the harmonic domain. This paper primarily proposes a transfer of some results and inverse-engineering techniques used to transport or launch trapped ions and neutral atoms—shortcuts to adiabaticity [14]—to design control operations for cranes. By establishing the link among the two fields, we also open the way for a reverse transfer, from the considerable body of work and results developed by engineers to control crane operation in the microscopic realm. Some examples of transfer are discussed in the final section. In the rest of the Introduction, we provide basic facts on cranes, as well as shortcuts to adiabaticity and their application to cranes based on invariants of motion.

A. Cranes

Cranes are mechanical machines that lift and transport loads by means of a hoisting rope supported by a structure that moves the suspension point. They range from gigantic versions in ports or special construction sites to minicranes and even microscopic, molecular-sized devices [15]. Exact forms and types (overhead, rotary, or boom cranes [13]) also vary widely to adapt to different applications, and they can be operated manually or automatically. In either case, standard objectives of the crane operation are to transport

*Corresponding author.
jg.muga@ehu.eus

the load in a short time, depositing it safely and at rest—or at least unexcited—at the final destination. Typically, the residual (final) pendulations are to be minimized, while larger pendulations are allowed on route as long as the safety of the operation is not at risk. The dynamical models are frequently linearized to apply linear control methods, as normal operation conditions involve small sway angles [13,16–20]. Open-loop (without feedback control) and closed-loop (with feedback provided by sensors) strategies have been proposed. The potential superiority of closed-loop approaches is overtaken by their difficult implementation, which requires accurate measurements during the operation, so that open-loop approaches are dominant in actual crane controllers [13]. Nevertheless, known problems of the open-loop approaches are their sensitivity with respect to different perturbations such as wind, damping, changes in initial conditions, or imperfect implementation of the control functions [13,21]. Moreover, optimal solutions often imply bang-bang (stepwise constant) acceleration profiles of control parameters, which are hard to implement and which generate stress on the structure [13].

B. Shortcuts to adiabaticity

Slow transformations of external parameters that control quantum systems allow us, in principle, to avoid excitations and, specifically, to reach ground states that could be difficult to achieve otherwise. These slow processes are, in principle, robust with respect to smooth changes of parameter paths but not necessarily with respect to rapid or noisy perturbations. There is a growing interest in accelerating these transformations to limit the detrimental effect of decoherence or noise, or to increase the number of operations that can be carried out in a given time interval [14]. Shortcuts to adiabaticity are methods that bypass slow adiabatic transformations via faster routes by designing appropriate time-dependent Hamiltonians. The shortcuts include methods based on exact solutions with scaling parameters [22–25] and on dynamical Lewis-Riesenfeld invariants [23,26,27], approaches that add "counterdiabatic" terms to the Hamiltonian [28–30], the "fast-forward" approach [31–38], Lie-algebraic methods [39,40], or the fast quasiadiabatic approach [41]. They all have applications beyond the quantum domain, see, e.g., applications in optics [5–9] and classical systems [24,38,42–45].

C. Invariants and cranes

Use of invariants of motion to inverse engineer the trolley trajectory and the rope length will allow us to design for the open-loop strategy (for closed-loop control, see Ref. [21]) robust, smooth protocols with respect to initial conditions: specifically, we shall generate a family of protocols that, by construction, produce at final time the adiabatic energy, namely, the energy that would be reached after an infinitely slow process. The fact that the solution for the time dependence of the protocol parameters is highly degenerate allows for further optimization, with respect to other physical variables or robustness, as demonstrated, e.g., in Refs. [26,46] within the microscopic domain. We demonstrate here the possibility of using the degeneracy to devise protocols that remain robust beyond the harmonic regime.

We shall also establish a minimal work principle for the system, which states generally that, on average, the adiabatic work done on the system or extracted from it for very slow processes is optimal. A brief history of the principle and its various formulations and derivations for specific systems and conditions is provided in Refs. [47,48]. For the present context, we shall prove it in Appendix A, considering a microcanonical ensemble of initial conditions of the payload, by generalizing the results in Ref. [49]. The relevance of the result is that invariant-based inverse engineering of the crane control parameters provides, for the microcanonical ensemble of initial conditions, the minimal possible final average energy with faster-than-adiabatic protocols.

Section II explains how to implement invariant-based inverse engineering for crane control, and Sec. III provides some examples, including a comparison of sequential versus dual approaches. The article ends with a discussion containing an outlook for future work and a demonstration of the possibility of going beyond the harmonic regime. Finally, appendixes are included on the maximal work principle, the derivation of the Hamiltonian in the small oscillations regime, and the expression for the exact adiabatic energy.

II. INVARIANT-BASED ENGINEERING OF CRANE CONTROL

Invariant-based engineering is the approach best adapted to the peculiarities of trapped ions and has been extensively applied by our group in that context [50–57]. Here, we propose an inverse-engineering method for crane operations based on the invariants of motion of the system. While the approach can be generalized and applied to different, complex crane types, to be specific, we set a simple overhead crane model with a horizontal fixed rail at height $z = 0$. A control trolley travels along the rail holding a hoist rope of controllable length l from $x = 0$ to $x = d$. We assume that the rope is rigid for a given length and also neglect its mass and damping, which are all standard approximations. Suppose that a point payload of mass m is to be moved from $0, z_0$ to d, z_f, with $z_0, z_f < 0$, in a time t_f. (We shall, in fact, allow for some deviation from the ideal equilibrium conditions).

For the rectilinear motion of the suspension point, transversal and longitudinal motions of the payload are uncoupled, so the dynamical problem is reduced to a two-dimensional vertical plane with coordinates $\{x, z\}$. Specifically, we assume that the initial and final rope lengths are chosen as

$$l(0) = l_0 = -z_0, \qquad l(t_f) = l_f = -z_f. \tag{1}$$

The Lagrangian for the payload is, in terms of the swing angle θ,

$$L = \frac{m}{2}(\dot{x}^2 + \dot{l}^2 + l^2\dot{\theta}^2 + 2\dot{x}\,\dot{l}\sin\theta + 2\dot{x}l\dot{\theta}\cos\theta) + mgl\cos\theta, \tag{2}$$

where the first line is the kinetic energy $\mathcal{T}$, and the second line is the negative of the potential energy, $-\mathcal{V}$. The corresponding dynamics, with $l(t)$ and $x(t)$ being external control functions, is given by

$$l\ddot{\theta} + 2\dot{l}\,\dot{\theta} + g\sin\theta + \ddot{x}\cos\theta = 0, \tag{3}$$

where one and two dots denote first- and second-order time derivatives, and g is the gravitational acceleration. Using as a new variable the horizontal deviation of the payload from the position of the trolley, $q = l\sin\theta$, and small oscillations, the kinematics of the load are described by the linear equation

$$\ddot{q} + \left(\frac{g}{l} - \frac{\ddot{l}}{l}\right)q = -\ddot{x}, \tag{4}$$

which corresponds to a forced harmonic oscillator with the squared, time-dependent angular frequency

$$\omega^2(t) = \frac{g}{l} - \frac{\ddot{l}}{l}. \tag{5}$$

We shall assume for a smooth operation that

$$\dot{l}(t_b) = \ddot{l}(t_b) = 0, \tag{6}$$

where we use the shorthand notation $t_b = 0, t_f$ for the (initial or final) boundary times. Specifically, the vanishing second derivative implies [see Eq. (5)] that

$$\omega^2(0) = \frac{g}{l_0}, \qquad \omega^2(t_f) = \frac{g}{l_f}. \tag{7}$$

In a moving frame, the kinematics in Eq. (4) may as well be derived from the Hamiltonian (the canonical transformations are given in Appendix B),

$$H = \frac{p^2}{2m} + \frac{m}{2}\omega^2(t)q^2 + m\ddot{x}q, \tag{8}$$

with $p = mdq/dt$, which has the invariant of motion [58]

$$I = \frac{1}{2m}[b(p - m\dot{\alpha}) - m\dot{b}(q-\alpha)]^2 + \frac{m}{2}\omega_0^2\left(\frac{q-\alpha}{b}\right)^2, \tag{9}$$

provided the scaling factor $b(t)$ and $\alpha(t)$ satisfy the Ermakov and Newton equations

$$\ddot{b} + \omega^2(t)b = \frac{\omega_0^2}{b^3}, \tag{10}$$

$$\ddot{\alpha} + \omega^2(t)\alpha = -\ddot{x}, \tag{11}$$

where ω_0 is, in principle, an arbitrary constant, but it is customary and convenient to take $\omega_0 = \omega(0)$. Note that Eqs. (4) and (11) have the same structure, corresponding to a forced oscillator. However, while Eq. (4) is general and applies to arbitrary boundary conditions for the trajectory, we shall choose $\alpha(t)$ functions that satisfy the boundary conditions

$$\alpha(t_b) = \dot{\alpha}(t_b) = \ddot{\alpha}(t_b) = 0. \tag{12}$$

These boundary conditions also imply [see Eq. (4)] that $\ddot{x}(t_b) = 0$. Moreover, for the boundary conditions of the scaling function, we choose

$$b(0) = 1, \quad b(t_f) = \gamma = \left(\frac{\omega_0}{\omega_f}\right)^{1/2}, \quad \dot{b}(t_b) = \ddot{b}(t_b) = 0, \tag{13}$$

where $\omega_f = \omega(t_f)$. $I(0)$ is equal to the initial energy of the payload $E_0 = p^2(0)/(2m) + (m/2)\omega_0^2 q^2(0)$, where $q(0)$ and $p(0)$ are arbitrary initial conditions. $I(t_f)$, which must be equal to E_0 since I is an invariant, takes the form $I(t_f) = \gamma^2 E_f$, where $E_f = p^2(t_f)/(2m) + (m/2)\omega_f^2 q^2(t_f)$ is the final energy, and $q(t_f)$ and $p(t_f)$ are found by solving Eq. (4) with the initial conditions $q(0)$, $p(0)$. [These energies correspond to the Hamiltonian (8), with zero potential at the equilibrium position $\theta = 0$ or $q = 0$. $H(t)$ is not, in general, equal to the shifted mechanical energy $\mathcal{T} + \mathcal{V} + mgl$, except at the boundary times.] In other words, for the processes defined by the auxiliary functions $\alpha(t)$ and $b(t)$ satisfying their stated boundary conditions, the final energy at time t_f is, for any initial energy E_0, the adiabatic energy $E_{\rm ad} = E_0\omega_f/\omega_0$, i.e., the one that could be reached after a slow evolution of the control parameters along an infinitely slow process. This result is very relevant since, as shown in Appendix A, the minimal final average energy, averaged over an initial microcanonical ensemble [a distribution of initial conditions proportional to Dirac's delta $\delta(E - E_0)$], is given by the adiabatic energy.

To inverse engineer the control parameters for a generic transport goal which involves simultaneous hoisting or lowering of the rope and trolley transport, we proceed as follows.

(i) $b(t)$ is interpolated between 0 and t_f leaving two free parameters. A simple choice is the polynomial form

$$b(t) = \sum_{j=0,7} a_j S^j = 1 + (-10 + 10\gamma - a_6 - 3a_7)S^3 + (15 - 15\gamma + 3a_6 + 8a_7)S^4 + 3(-2 + 2\gamma - a_6 - 2a_7)S^5 + a_6 S^6 + a_7 S^7, \quad (14)$$

where the values of a_j, $j < 6$, are fixed by the boundary conditions (13), and $S \equiv t/t_f$.

(ii) The corresponding squared frequency $\omega^2(t; a_6, a_7)$ is deduced from the Ermakov equation (10).

(iii) The two free parameters in $b(t; a_6, a_7)$ are fixed by solving Eq. (5) with initial conditions $l(0) = l_0, \dot{l}(0) = 0$ [$\ddot{l}(0) = 0$ is automatically satisfied according to Eq. (5)], so that the final conditions are $l(t_f) = l_f, \dot{l}(t_f) = 0$ [again, $\ddot{l}(t_f) = 0$ is satisfied automatically]. Multiple solutions are, in principle, possible because the system is nonlinear. We use a root-finding subroutine (FINDROOT by *Mathematica*) starting with the seed $a_6 = a_7 = 0$ to specify the form of $l(t)$ and $\omega(t)$.

(iv) A functional form for $\alpha(t)$ is used satisfying the boundary conditions (12) with two free parameters. Again, a polynomial is a simple, smooth choice,

$$\alpha(t) = \sum_{j=0,7} b_j S^j = -(b_6 + 3b_7)S^3 + (3b_6 + 8b_7)S^4 - 3(b_6 + 2b_7)S^5 + b_6 S^6 + b_7 S^7. \quad (15)$$

The trajectory of the trolley is deduced from Eq. (11) as

$$x(t) = -\int_0^t dt' \int_0^{t'} dt''[\ddot{\alpha}(t'') + \omega^2(t)\alpha], \quad (16)$$

which satisfies $\ddot{x}(t_b) = \dot{x}(0) = x(0) = 0$. The two free parameters in $\alpha(t; b_6, b_7)$ are set by demanding

$$x(t_f) = d, \qquad \dot{x}(t_f) = 0. \quad (17)$$

Compare the above sequence to a simpler inverse approach in which $l(t)$ is designed to satisfy Eqs. (1) and (6) so as to get $\omega(t)$ from Eq. (5), and $\alpha(t)$ then is designed to satisfy the conditions in Eq. (12). In this simpler approach, $b(t)$ is not engineered, which means that, in general, it will not satisfy the boundary conditions in Eq. (13), and, as a consequence, a vanishing residual excitation (with respect to the adiabatic energy) is only guaranteed for a $q(t)$ that satisfies the initial boundary conditions in Eq. (12). In other words, the extra effort to design $b(t)$ leads by construction [see Eq. (9)] to the adiabatic energy at the final time for any initial boundary conditions $q(0), \dot{q}(0)$.

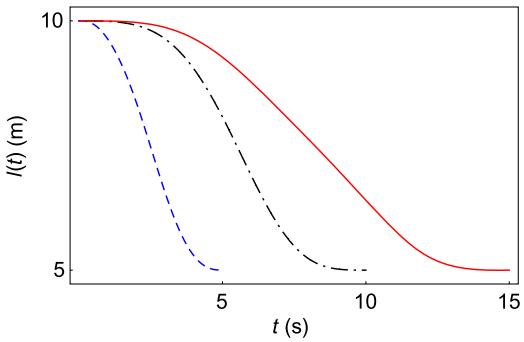

FIG. 1. Length of the rope with respect to time for a hoisting from $l_0 = 10$ m to $l_f = 5$ m. $t_f = 15$ s, red solid line; $t_f = 10$ s, black dashed-dotted line; and $t_f = 5$ s, blue dashed line.

III. NUMERICAL EXAMPLES

In this section, we show some examples of crane operation and payload behavior following the inverse-engineering protocol described in steps (i)–(iv). Figures 1 and 2 show the control functions $l(t)$ and $x(t)$ found for different final times, with parameters $d = 15$ m, $l_0 = 10$ m, and $l_f = 5$ m. Figure 3 shows the swing angle of the payload with respect to time for these protocols, with the payload initially set at equilibrium. It is calculated exactly (with the full Lagrangian) for different final times, and also with the approximate equation for small oscillations (4), but the difference is noticeable only for the smallest time, $t_f = 5$ s. Clearly, short times imply larger transient angles, so larger errors may be expected as the small-oscillation regime is abandoned. To quantify the error, we plot in Fig. 4 the maximal angle of the payload in the final configuration, $\theta_{\max}(t_f)$—i.e., the maximal angle for the pendulations with $l = l_f$ once the trolley has reached the final point d and remains at rest—versus the initial angle [with $\dot{\theta}(0) = 0$]. The maximal angle is, of course, related to the exact final energy, given [since

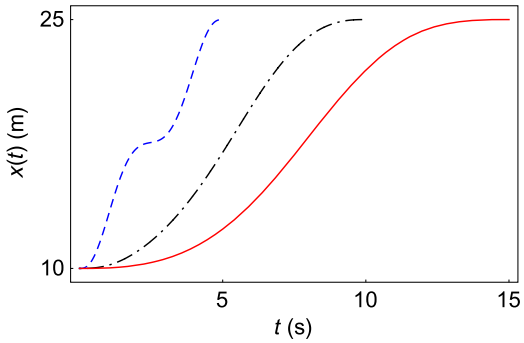

FIG. 2. Position of the trolley $x(t)$ with respect to time for a dual operation with $d = 15$, $l_0 = 10$ m, and $l_f = 5$ m. $t_f = 15$ s, red solid line; $t_f = 10$ s, black dashed-dotted line; and $t_f = 5$ s, blue dashed line.

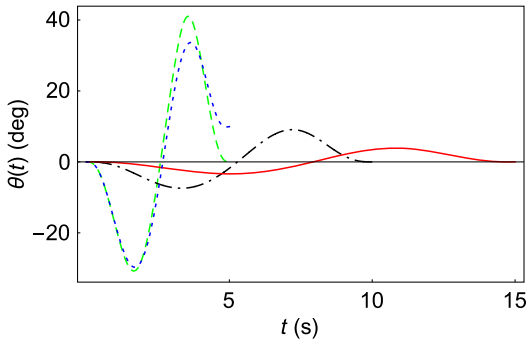

FIG. 3. Angle of the payload with respect to time for a dual operation with a translation of 15 m and a hoisting from $l_0 = 10$ m to $l_f = 5$ m). The exact dynamics are $t_f = 15$ s, red solid line; $t_f = 10$ s, black dashed-dotted line; and $t_f = 5$ s, blue dotted line. The approximate dynamics (harmonic approximation) are $t_f = 5$ s, green dashed line; for the two other times, the exact and approximate curves are undistinguishable in the scale of the figure. The payload is initially set at equilibrium.

$\dot{l}(t_f) = \dot{x}(t_f) = 0]$ by $E_f = mgl(1 - \cos[\theta_{\max}(t_f)])$. In Fig. 4, we compare this final maximal angle to the maximal angle that would be found adiabatically after an infinitely slow process. The exact adiabatic angle can be calculated as explained in Appendix C. The figure demonstrates that hoisting the payload (cable shortening) leads to larger maximal angles than lowering it does.

A. Sequential versus dual

A global process that includes transport and hoisting or lowering can be done performing the two operations simultaneously, as described above (dual operation), but also sequentially, performing one operation at a time [20].

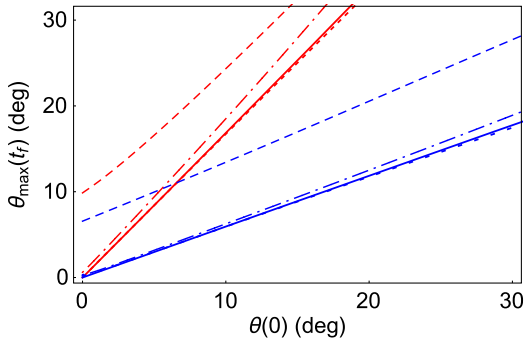

FIG. 4. Maximal angle of the payload in the final configuration versus the initial angle for a payload initially at rest, $\dot{\theta}(0) = 0$. For the same line type, the (red) curve with a larger slope corresponds to transport with hoisting ($l_0 = 10$ m, $l_f = 5$ m, and $d = 15$ m) and the other (blue) curve to transport with lowering ($l_0 = 5$ m, $l_f = 10$ m, and $d = 15$ m). The solid lines are the (exact) adiabatic lines. $t_f = 10$ s, dotted lines; $t_f = 7$ s, dashed-dotted lines; and $t_f = 5$ s, dashed lines.

Which of the two possibilities is faster? For the analogous problem consisting of atom transport or launching combined with trap expansions, we found that the answer depends critically on the constraints and parameters imposed [59]. In the current setting, we shall also demonstrate through examples that, by imposing some constraints, either the dual or the sequential approach could be faster depending on the parameter values chosen. A dual protocol is not just the simultaneous superposition of the two sequential operations: While $l(t)$ is indeed the same in the dual and hoisting or lowering part of the sequential process [the first three steps, (i)–(iii), would be identical], $x(t)$ is different in the dual process and in the pure-transport segment of the sequential process, where l is constant. This is the case because, in Eq. (11), the time dependence of the angular frequency affects the design of $\alpha(t)$ and $x(t)$.

Consider processes where the trolley moves from 0 to d with a lowering from l_0 to $l_f > l_0$. We assume the initial conditions $q(0) = \dot{q}(0) = \ddot{q}(0) = 0$ [which implies $q(t) = \alpha(t)$; see Eqs. (4) and (11)], and the protocols for the control functions using the polynomial *Ansätze* described above. We impose that the protocols should satisfy three constraints: $-10 \le \theta(t) \le 10$ may be imposed for a safe operation and guarantees the validity of the harmonic model, and $0 \le x(t) \le d$ and $0 \le l \le l_f$ are the assumed geometrical constraints on the trolley trajectory and cable length. Of course, other geometries may also be considered. For example, the presence of obstacles may imply the necessity of a sequential approach.

Table I shows the minimal times found for different cases. In all, $l_0 = 5$ m and $l_f > l_0$, and the protocols are found according to the steps described above. The fastest protocol may be dual or sequential depending on the

TABLE I. Minimal times for sequential and dual protocols with different parameters. $\Delta l = l_f - l_0$, with $l_0 = 5$ m for all cases. Times for the sequential process are divided into minimal times for pure transport and pure lowering processes. The footnotes indicate the constraints that set the minimal time. The transport in the last row has two minimal times because pure transport with l_0 and with l_f are bounded by different constraints. In all other cases, the constraint is the same for both lengths, so they share the same minimal time; see the main text.

		Sequential time (s)			Dual time (s)
d (m)	Δl (m)	Transport	Lowering	Total	
15	5	9.1[a]	1.29[b]	10.39	9.55[a]
15	30	9.1[a]	1.16[b]	10.26	10.7[a]
50	30	16.6[a]	1.16[b]	17.76	21[a]
5	50	5.25[a] (l_0) 7.76[c] (l_f)	1.1[b]	6.35 (l_0) 8.86 (l_f)	7[a]

[a]Constraint $-10 \le \theta(t) \le 10$.
[b]Constraint $0 \le l(t) \le l_f$.
[c]Constraint $0 \le x(t) \le d$.

parameters chosen. However, in the last line, the minimal time for the sequential approach is the same regardless of the order in which the two operations (pure transport and pure lowering) are performed. In other words, the minimal time for transport is the same for l_0 or l_f. Notice that, for a constant ω value, the free parameters in $\alpha(t; b_6, b_7)$, fixed so that boundary conditions in Eq. (17) are satisfied, are explicitly given by

$$b_6 = \frac{17640d}{t_f^2\omega^2}, \qquad b_7 = -\frac{5040d}{t_f^2\omega^2}, \tag{18}$$

which yields the scaling $\omega_0^2\alpha_0(t) = \omega_f^2\alpha_f(t)$, where $\alpha_0(t)$ and $\alpha_f(t)$ correspond to transport with l_0 and l_f, respectively. Using Eq. (5) (with $\ddot{l} = 0$), it is found that

$$\frac{\alpha_0(t)}{l_0} = \frac{\alpha_f(t)}{l_f}, \tag{19}$$

which means that the triangle formed by the cable of length l_0, the horizontal displacement $\alpha_0(t)$, and the vertical is similar to the triangle formed by l_f, $\alpha_f(t)$, and the vertical. Thus, the evolution of the angle $\theta(t)$ is independent of the rope length in these protocols.

This symmetry is broken in the last line of Table I because the transport function with an l_f value similar to the transport process that gives the minimal time with l_0 violates the constraint imposed on $x(t)$. We then have to increase the process time until the constraint is satisfied, so Eq. (19) does not apply.

IV. DISCUSSION

Analogies among disparate systems provide opportunities for a fruitful interchange of techniques and results. Here, we work out an invariant-based inverse-engineering approach to control crane operations, which had been applied previously to control the transport of atoms and ions. We provide protocols that guarantee final adiabatic energies, which are shown to be minimal when averaging over a microcanonical ensemble of initial conditions. Natural applications of these protocols would be in robotic cranes with good control of the driving parameters and uncertainties in the initial conditions.

Several results in the microscopic domain may be translated to crane control. Here are some examples of possible connections for future work.

(a) In Ref. [25], the excess final energy in transport processes was related to a Fourier transform of the acceleration of the trap. By a clever choice of acceleration function, it is possible to set a robustness window for the trap frequency. In the context of cranes, this window provide robustness with respect to rope length in transport operations.

(b) A more realistic treatment of the crane implies a double pendulum [18]. Setting the shortcuts in that case will require considering two harmonic oscillators, by means of a dynamical normal-mode analysis similar to the one done for two ions [57].

(c) Invariant-based inverse-engineering combines well with optimal control theory [60–62]. The main point is that the shortcut design guarantees a final excitation-free state but leaves room to choose the control parameters so as to optimize some relevant variable, typically for a bounded domain of values for the control parameters. Results found for microscopic systems to minimize times or transient energies can be applied to crane systems.

(d) Noise and perturbations, including anharmonicities, may be treated perturbatively to minimize their effect, as in Refs. [26,63].

An alternative practical scheme for dealing with anharmonicity (i.e., nonlinear effects beyond the small-oscillation regime) was put forward in Ref. [64]: Instead of using a minimum set of parameters to the design of the auxiliary functions (α and b), *Ansätze* with additional parameters enable us to minimize the final excitation for a broad domain of initial angles. In Fig. 5, we depict ratios of final to initial energies for a pure-transport process. One of the protocols

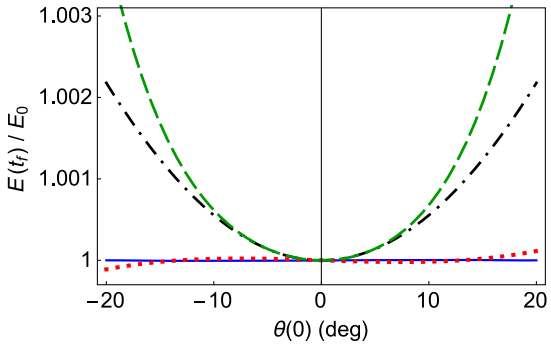

FIG. 5. Final-to-initial-energy ratio for pure transport (no hoisting involved) versus the initial angle for a load initially at rest. Here, the initial energy is equal to the final adiabatic energy, as the cable length does not change. Protocols are as follows: (i) the three-step protocol in Ref. [65] in the harmonic approximation (the black dotted-dashed line) and for the exact dynamics (the green dashed line), (ii) an invariant-based protocol (the red dotted line) with a polynomial *Ansatz* (15) for α (the blue solid line in the harmonic approximation, the red dotted line for the exact dynamics), and (iii) an invariant-based protocol with three more parameters in the polynomial adjusted to flatten the excitation curve as in Ref. [64] (the blue solid line, indistinguishable from 1 in the scale of the figure throughout the entire angle interval). The parameters are taken from Ref. [65]: $l = 1.2$ m and $x_f = 4$ m. The upper bounds to set the protocol (i) for trolley acceleration, trolley velocity, and payload angle are (the notation is the one in [65]): $a_{\rm ub} = 0.5$ m/s^2, $v_{\rm ub} = 1$ m/s, $\theta_{\rm ub} = 5°$. These parameters imply a total time $t_f = 6.45$ s with $a_{\rm max} = 0.4276$ m/s^2, $T = 2.1987$ s, and $t_c = 2.0567$ s. All protocols are adjusted for the same final total time.

used was devised in Ref. [65] in the harmonic regime to set the load at rest at the final time when starting at $\theta(0)=0$, $\dot{\theta}(0)=0$ by three steps with constant (stepwise) acceleration: $a_{\max}$ during an oscillation period T, coasting (constant velocity) for t_c, and $-a_{\max}$ for a time T. $a_{\max}$ and t_c are chosen to satisfy imposed upper bounds on the swing angle $\theta_{\rm ub}$, the acceleration $a_{\rm ub}$, and the velocity $v_{\rm ub}$ for the trolley. The values, taken from an example in Ref. [65], are given in the caption. The ratio grows from 1 as the initial angle increases, even in the harmonic approximation (the black dotted-dashed line). The exact results give even higher values (the green dashed line). By contrast, the invariant-based protocol using $b(t)=1$ and the polynomial *Ansatz* for α, Eq. (15), with parameter values to satisfy Eqs. (12) and (17), gives no excitation at all in the harmonic approximation (this is the case by construction; see the blue solid line), and little excitation when using the exact dynamics (the red dotted line). The result can be made even better by increasing the order of the polynomial for α and using the free parameters to minimize the total excitation at a grid of selected initial angles; see Ref. [64]. Choosing three more parameters and the angles $\theta(0)=-20,-15,15,20$, the energy ratio becomes indistinguishable from 1.

We end with an important example of a positive influence in the opposite direction, from the macroscopic to the microscopic realm. The analysis of energy management and expenditure has been more realistic in engineering publications (see, e.g., Ref. [20]) than in the work on microscopic systems. A useful energy cost analysis of a shortcut must include the control system (the trolley) in addition to the primary system (the payload). In Ref. [64], the dynamics of the crane is analyzed in terms of coupled dynamical equations for the trolley and the payload [20] for a transport operation (with a constant l),

$$0=l\ddot{\theta}+\ddot{x}\cos\theta+g\sin\theta, \tag{20}$$

$$\mathcal{F}_a+\mathcal{F}_r=M\ddot{x}+m(\ddot{x}+l\ddot{\theta}\cos\theta-l\dot{\theta}^2\sin\theta), \tag{21}$$

where M is the mass of the trolley, $\mathcal{F}_a(t)$ an actuating force (due to an engine or braking), and $\mathcal{F}_r$ a friction force, simply modeled as $\mathcal{F}_r=-\Gamma\dot{x}$, $\Gamma\geq 0$. In contrast to Eq. (3), the trolley position is now regarded as a dynamical variable. To achieve a given form $x(t)$, as specified by the inverse-engineering approach, $\mathcal{F}_a(t)$ must be modulated accordingly, so it will depend on the specified $x(t)$, the trolley characteristics (mass M and friction coefficient Γ), and the payload dynamics and characteristics. The power due to the actuating force, $\mathcal{P}=\mathcal{F}_a\dot{x}$, may be easily translated into fuel, or electric power consumption, and is, in general, quite different from the power computed as the time derivative of the mechanical energy of the payload alone. It takes, for small oscillations, the simple form

$$\mathcal{P}=\mathcal{F}_a\dot{x}=(M\ddot{x}-mq\omega^2+\Gamma\dot{x})\dot{x}, \tag{22}$$

whose peaks and time integrals were studied in Ref. [64], with different treatments for different braking mechanisms. The energy cost of shuttling neutral atoms in optical traps moved by motorized motions of mirrors or lenses [66,67] may, in fact, be analyzed in the same manner, as the shortcut design is based on exactly the same equations.

ACKNOWLEDGMENTS

We acknowledge our discussions with S. Martínez-Garaot and M. Palmero. This work was supported by Eusko Jaurlaritza (Grant No. IT986-16); MINECO/FEDER,UE (Grants No. FIS2015-67161-P and No. FIS2015-70856-P); QUITEMAD+CM S2013-ICE2801; and by Programme Investissements d'Avenir under the program ANR-11-IDEX-0002-02, reference ANR-10-LABX-0037-NEXT.

APPENDIX A: MINIMAL WORK

Here, we follow closely Ref. [49]; the main difference is that we allow for a harmonic Hamiltonian with a homogeneous, time-dependent force $F(t)$,

$$H=p^2/2m+\frac{m}{2}\omega^2(t)q^2-F(t)q, \tag{A1}$$

which, we assume, will satisfy $F(0)=F(t_f)=0$. Consider the area-preserving phase-flow map between the initial and final values of the position and momentum,

$$\Phi:\begin{pmatrix}q_0\\p_0\end{pmatrix}\rightarrow\begin{pmatrix}q_f\\p_f\end{pmatrix}, \tag{A2}$$

$$\Phi=\begin{pmatrix}a&b\\c&d\end{pmatrix}, \tag{A3}$$

where $\det(\Phi)=1$. In terms of the matrix elements of Φ, the final energy for the initial conditions q_0, p_0 with energy E_0 is

$$E_f=E_0(\alpha\cos^2\phi+\beta\sin^2\phi+\eta\sin 2\phi), \tag{A4}$$

where

$$\alpha=\frac{c^2}{m^2\omega_0^2}+a^2\frac{\omega_f^2}{\omega_0^2},\qquad \beta=d^2+\omega_f m^2b^2, \tag{A5}$$

$$\eta=\frac{cd}{m\omega_0}+abm\frac{\omega_f^2}{\omega_0}, \tag{A6}$$

and the angle ϕ is introduced as

$$q_0=\sqrt{\frac{2E_0}{m\omega_0^2}}\cos\phi,\qquad p_0=\sqrt{2mE_0}\sin\phi. \tag{A7}$$

For a uniform (microcanonical) distribution of initial angles, $P(\phi) = 1/(2\pi)$, the average final energy is

$$\overline{E}_f = \frac{1}{2\pi}\int E_f d\phi = \frac{E_0}{2}(\alpha+\beta). \tag{A8}$$

This result gives for the variance

$$\mu^2 \equiv \overline{(E_f - \overline{E}_f)^2} = \frac{E_0^2}{2}\left[\left(\frac{\overline{E}_f}{E_0}\right)^2 - \frac{\omega_f^2}{\omega_0^2}\right], \tag{A9}$$

so $\overline{E}_f \geq E_0(\omega_f/\omega_0)$, i.e., the final averaged energy is greater than or equal to the adiabatic energy at t_f, $E_{\rm ad} = E_0\omega_f/\omega_0$.

APPENDIX B: DETAILED DERIVATION OF THE HAMILTONIAN

To derive the Hamiltonian (8), let us first rewrite it in a slightly more detailed notation as

$$H_q = \frac{p_q^2}{2m} + \frac{m}{2}\left(\frac{g}{l} - \frac{\ddot{l}}{l}\right)q^2 + mq\ddot{x}. \tag{B1}$$

1. Lagrangian and Hamiltonian in θ

The starting point is the Lagrangian of the system in the θ variable, Eq. (2). Let us define the conjugate momentum p_θ as

$$p_\theta = \frac{\partial L}{\partial\dot{\theta}} = ml^2\dot{\theta} + ml\dot{x}\cos\theta. \tag{B2}$$

We now define the Hamiltonian as the Legendre transform of the Lagrangian by writing everything in terms of θ and p_θ,

$$\begin{aligned} H_\theta &= \dot{\theta}p_\theta - L \\ &= \frac{p_\theta^2}{2ml^2} - mgl\cos\theta - \frac{\dot{x}\cos\theta}{l}p_\theta \\ &\quad - \frac{1}{2}m(\dot{x}^2\sin^2\theta + 2\dot{l}\,\dot{x}\sin\theta), \end{aligned} \tag{B3}$$

where we omit terms that do not depend on θ or p_θ so that they do not affect the dynamics.

2. Horizontal deviation Q: Change of coordinate

We look for a canonical transformation to $\{Q, p_Q\}$ variables such that the new coordinate is the horizontal deviation from the suspension point $Q = l\sin\theta$. This transformation is achieved with the (time-dependent) generating function $F_2 = p_Q l\sin\theta$.F_2 generates the desired change of coordinate since

$$Q = \frac{\partial F_2}{\partial p_Q} = l\sin\theta, \tag{B4}$$

$$p_\theta = \frac{\partial F_2}{\partial\theta} = p_Q l\cos\theta. \tag{B5}$$

Including the inertial effects given by $\partial_t F_2 = p_Q\dot{l}\sin\theta = p_Q Q\dot{l}/l$, the Hamiltonian in the new variables is

$$\begin{aligned} H_Q &= \frac{p_Q^2}{2m}\left(1 - \frac{Q^2}{l^2}\right) - mgl\sqrt{1 - \frac{Q^2}{l^2}} - \frac{m\dot{l}\,\dot{x}}{l}Q \\ &\quad - \frac{m\dot{x}^2}{2l^2}Q^2 + \frac{\dot{x}}{l^2}p_Q Q^2 + p_Q\left(\frac{\dot{l}}{l}Q - \dot{x}\right). \end{aligned} \tag{B6}$$

3. Momentum shift

The last term introduces a quadratic coordinate-momentum coupling and a linear-in-momentum term. To get rid of this term, we make a momentum shift by a second canonical transformation using the generating function

$$F_2' = Qp_q + m\dot{x}Q - \frac{m\dot{l}}{2l}Q^2. \tag{B7}$$

The transformation equations to the new canonical variables $\{q, p_q\}$ are

$$q = \frac{\partial F_2'}{\partial p_q} = Q, \tag{B8}$$

$$p_Q = \frac{\partial F_2'}{\partial Q} = p_q + m\dot{x} - \frac{m\dot{l}}{l}Q. \tag{B9}$$

Including the inertial effects

$$\partial_t F_2' = -\frac{mQ^2\ddot{l}}{2l} + \frac{mQ^2\dot{l}^2}{2l^2} + m\ddot{x}Q, \tag{B10}$$

the transformed Hamiltonian in the q and p_q variables is given by

$$\begin{aligned} H_q &= \frac{p_q^2}{2m}\left(1 - \frac{q^2}{l^2}\right) - mgl\sqrt{1 - \frac{q^2}{l^2}} + m\ddot{x}q - \frac{m\ddot{l}}{2l}q^2 \\ &\quad - \frac{m\dot{l}^2}{2l^4}q^4 + \frac{\dot{l}}{l^3}p_q q^3, \end{aligned} \tag{B11}$$

where, again, terms that do not affect the dynamics have been omitted.

4. Small oscillations

In the $q \ll l$ limit, keeping only quadratic terms in the coordinate and the momentum and continuing up through terms that do not affect the dynamics, the above Hamiltonian may be approximated by Eq. (B1). The next order is quartic (there is no cubic term),

$$V = \left(\frac{gm}{8l^3} - \frac{m\dot{l}^2}{2l^4}\right)q^4 - \frac{p_q^2 q^2}{2ml^2} + \frac{\dot{l}}{l^3}p_q q^3. \quad \text{(B12)}$$

Using the relations between momenta p_q, p_Q, and p_θ [see Eqs. (B5) and (B9)], p_q can be written in terms of the original coordinates θ and $\dot{\theta}$,

$$p_q = m(l\dot{\theta}\sec\theta + \dot{l}\sin\theta) \approx m(l\dot{\theta} + \dot{l}\theta) = m\frac{d(l\theta)}{dt}. \quad \text{(B13)}$$

In other words, in the small-oscillation regime where $q = l\sin\theta \approx l\theta$, the momentum p_q tends to $p_q \approx m\dot{q}$.

APPENDIX C: EXACT ADIABATIC MAXIMAL ANGLE

We shall determine the exact adiabatic maximal final angle of the payload. "Exact" here means that we do not use the harmonic approximation to calculate it. It would be the maximal angle for the final cable length and a given initial length and energy, after a very slow process. The maximal angle depends on the energy, so we first need an exact expression of the energy at the boundary times for an arbitrary process where the boundary conditions $\dot{l} = \dot{x} = \ddot{l} = \ddot{x} = 0$ are imposed. Using the exact Lagrangian (2) and θ as the generalized coordinate, so that $p_\theta = \partial L/\partial\dot{\theta}$, we find by a Legendre transformation

$$\tilde{E} = \frac{p_\theta^2}{2ml^2} - mgl\cos\theta, \quad \text{(C1)}$$

where the tilde in $\tilde{E}$ indicates that the zero of the potential energy corresponds here, unlike the definition in the main text based on Eq. (8), to $\theta = \pi/2$ and $l = l_0, l_f$. The maximum angle $\theta_{\max}$ for the boundary configurations, not to be confused with the angles at boundary times $\theta(0)$ or $\theta(t_f)$, is given by

$$\cos\theta_{\max} = -\frac{\tilde{E}}{mgl}. \quad \text{(C2)}$$

The adiabatic invariant [68], which is the phase-space area along an oscillation cycle, with l fixed, is given at the boundary times by

$$\begin{aligned} A(l,\theta_{\max}) &= 4\int_0^{\theta_{\max}} p_\theta d_\theta \\ &= 4\sqrt{2ml}\int_0^{\theta_{\max}} \sqrt{\tilde{E} + mgl\cos\theta}\,d\theta \\ &= 8\sqrt{2}ml^{3/2}\sqrt{1-\cos\theta_{\max}}\,\mathbf{E}\left(\frac{\theta_{\max}}{2}\middle|\frac{2}{1-\cos\theta_{\max}}\right), \end{aligned} \quad \text{(C3)}$$

where $\mathbf{E}$ is the incomplete elliptic integral of the second kind [69,70]. The exact final adiabatic maximum angle $\theta_{\max}(t_f)$ is found by imposing the equality of areas at the boundary times,

$$A[l_0, \theta_{\max}(0)] = A[l_f, \theta_{\max}(t_f)], \quad \text{(C4)}$$

where the initial maximum angle $\theta_{\max}(0)$ is found from the initial energy via Eq. (C2). The final adiabatic energy can be also obtained from Eq. (C2). As a consistency check, using the following properties of the elliptic integral [69,71],

$$\mathbf{E}(u|v) = v^{1/2}\mathbf{E}(uv^{1/2}|v^{-1}) - (v-1)u, \quad \text{(C5)}$$

$$\mathbf{E}(z|x) \sim z - \frac{2z - \sin(2z)}{8}x, \quad \text{as } x \sim 0, \quad \text{(C6)}$$

and the alternative convention for the zero of the energy, $E = \tilde{E} + mgl$, Eq. (C4) leads to the expected result $E_f = E_0\omega_f/\omega_0$ in the limit of small oscillations. For an arbitrary process, the actual final maximal angle and the corresponding energy will differ from the adiabatic values, as Fig. 4 demonstrates.

[1] U.S. Interagency Working Group on Quantum Information Science of the Subcommittee on Physical Sciences, "Advancing Quantum Information Science: National Challenges and Opportunities", National Science and Technology Council, 2016.

[2] C. Monroe, W. C. Campbell, E. E. Edwards, R. Islam, D. Kafri, S. Korenblit, A. Lee, P. Richerme, C. Senko, and J. Smith, in Quantum Simulation of Spin Models with Trapped Ions, *Proceedings of the International School of Physics "Enrico Fermi"*, Course CLXXXIX (Italian Physical Society, Bologna, 2015), p. 169.

[3] E. Torrontegui, A. Rauschhaut, D. Guéry-Odelin, and J. G. Muga, Simulation of quantum collinear chemical reactions with ultracold atoms, J. Phys. B **44**, 195302 (2011).

[4] A. Y. Smirnov, S. Savel'ev, L. G. Mourokh, and F. Nori, Modelling chemical reactions using semiconductor quantum dots, Europhys. Lett. **80**, 67008 (2007).

[5] S.-Y. Tseng and X. Chen, Engineering of fast mode conversion in multimode waveguides, Opt. Lett. **37**, 5118 (2012).

[6] S. Martínez-Garaot, S.-Y. Tseng, and J. G. Muga, Compact and high conversion efficiency mode-sorting asymmetric *Y* junction using shortcuts to adiabaticity, Opt. Lett. **39**, 2306 (2014).
[7] T.-H. Pan and S.-Y. Tseng, Short and robust silicon mode (de)multiplexers using shortcuts to adiabaticity, Opt. Express **23**, 10405 (2015).
[8] X. Chen, R.-D. Wen, and S.-Y. Tseng, Analysis of optical directional couplers using shortcuts to adiabaticity, Opt. Express **24**, 18322 (2016).
[9] S. Martínez-Garaot, J. G. Muga, and S.-Y. Tseng, Shortcuts to adiabaticity in optical waveguides using fast quasiadiabatic dynamics, Opt. Express **25**, 159 (2017).
[10] J. C. Maxwell, *An Elementary Treatise on Electricity*, 2nd ed. (Dover, New York, 2005), p. 51.
[11] D. J. Wineland, C. Monroe, W. M. Itano, D. Leibfried, B. E. King, and D. M. Meekhof, Experimental issues in coherent quantum-state manipulation of trapped atomic ions, J. Res. Natl. Inst. Stand. Technol. **103**, 259 (1998).
[12] D. Kielpinski, C. Monroe, and D. J. Wineland, Architecture for a large-scale ion-trap quantum computer, Nature (London) **417**, 709 (2002).
[13] E. M. Abdel-Rahman, A. H. Nayefh, and Z. N. Masoud, Dynamics and control of cranes: A review, J. Vib. Control **9**, 863 (2003).
[14] E. Torrontegui, S. Ibañez, S. Martínez-Garaot, M. Modugno, A. del Campo, D. Guéry-Odelin, A. Ruschhaupt, X. Chen, and J. G. Muga, Shortcuts to adiabaticity, Adv. At. Mol. Opt. Phys. **62**, 117 (2013).
[15] S. Kassem, A. T. L. Lee, D. A. Leigh, A. Markevicius, and J. Solà, Pick-up, transport and release of a molecular cargo using a small-molecule robotic arm, Nat. Chem. **8**, 138 (2016).
[16] S. C. Kang and E. Miranda, in *Proceedings of the Xth International Conference on Computing in Civil and Building Engineering (ICCCBE), Weimar, Germany 2004*, edited by K. Beucke, B. Firmenich, D. Donath, R. Fruchter, and K. Roddis (Bauhaus-Universität, Weimar, 2004), https://e-pub.uni-weimar.de/opus4/frontdoor/index/index/docId/231.
[17] J. B. Klaassens, G. E. Smid, H. R. van Nauta Lemke, and G. Honderd, in *Proceedings of the Second Annual Conference on Developments in Container Handling Automation and Technologies, London, 2000* (Cargo Systems, London, 2000), p. 1–17.
[18] T.-Y. T. Kuo and S.-C. J. Kang, Control of fast crane operation, Automation in Construction **42**, 25 (2014).
[19] H.-S. Liu and W.-M. Cheng, The motion planning of overhead crane based on suppressing payload residual swing, MATEC Web Conf. **40**, 02001 (2016).
[20] Z. Wu and X. Xia, Optimal motion planning for overhead cranes, IET Control Theory Appl. **8**, 1833 (2014).
[21] M. Zhang, X. Ma, X. Rong, X. Tian, and Y. Li, Error tracking control for underactuated overhead cranes against arbitrary initial payload swing angles, Mech. Syst. Signal Process. **84**, 268 (2017).
[22] J. G. Muga, X. Chen, A. Ruschhaupt, and D. Guéry-Odelin, Frictionless dynamics of Bose-Einstein condensates under fast trap variations, J. Phys. B **42**, 241001 (2009).
[23] X. Chen, A. Ruschhaupt, S. Schmidt, A. del Campo, D. Guéry-Odelin, and J. G. Muga, Fast Optimal Frictionless Atom Cooling in Harmonic Traps, Phys. Rev. Lett. **104**, 063002 (2010).
[24] D. Guéry-Odelin, J. G. Muga, M. J. Ruiz-Montero, and E. Trizac, Exact Nonequilibrium Solutions of the Boltzmann Equation under a Time-Dependent External Force, Phys. Rev. Lett. **112**, 180602 (2014).
[25] D. Guéry-Odelin and J. G. Muga, Transport in a harmonic trap: Shortcuts to adiabaticity and robust protocols, Phys. Rev. A **90**, 063425 (2014).
[26] A. Ruschhaupt, X. Chen, D. Alonso, and J. G. Muga, Optimally robust shortcuts to population inversion in two-level quantum systems, New J. Phys. **14**, 093040 (2012).
[27] S. Martínez-Garaot, E. Torrontegui, X. Chen, M. Modugno, D. Guéry-Odelin, Shuo-Yen Tseng, and J. G. Muga, Vibrational Mode Multiplexing of Ultracold Atoms, Phys. Rev. Lett. **111**, 213001 (2013).
[28] M. Demirplak and S. A. Rice, On the consistency, extremal, and global properties of counterdiabatic fields, J. Chem. Phys. **129**, 154111 (2008).
[29] M. V. Berry, Transitionless quantum driving, J. Phys. A **42**, 365303 (2009).
[30] X. Chen, I. Lizuain, A. Ruschhaupt, D. Guéry-Odelin, and J. G. Muga, Shortcut to Adiabatic Passage in Two- and Three-Level Atoms, Phys. Rev. Lett. **105**, 123003 (2010).
[31] S. Masuda and K. Nakamura, Fast-forward of adiabatic dynamics in quantum mechanics, Proc. R. Soc. A **466**, 1135 (2010).
[32] S. Masuda and K. Nakamura, Acceleration of adiabatic quantum dynamics in electromagnetic fields, Phys. Rev. A **84**, 043434 (2011).
[33] E. Torrontegui, S. Martínez-Garaot, A. Ruschhaupt, and J. G. Muga, Shortcuts to adiabaticity: Fast-forward approach, Phys. Rev. A **86**, 013601 (2012).
[34] E. Torrontegui, S. Martínez-Garaot, M. Modugno, X. Chen, and J. G. Muga, Engineering fast and stable splitting of matter waves, Phys. Rev. A **87**, 033630 (2013).
[35] S. Masuda, K. Nakamura, and A. del Campo, High-Fidelity Rapid Ground-State Loading of an Ultracold Gas into an Optical Lattice, Phys. Rev. Lett. **113**, 063003 (2014).
[36] K. Takahashi, Unitary deformations of counterdiabatic driving, Phys. Rev. A **91**, 042115 (2015).
[37] S. Deffner, Shortcuts to adiabaticity: Suppression of pair production in driven Dirac dynamics, New J. Phys. **18**, 012001 (2016).
[38] C. Jarzynski, S. Deffner, A. Patra, and Y. Subasi, Fast forward to the classical adiabatic invariant, Phys. Rev. E **95**, 032122 (2017).
[39] S. Martínez-Garaot, E. Torrontegui, Xi Chen, and J. G. Muga, Shortcuts to adiabaticity in three-level systems using Lie transforms, Phys. Rev. A **89**, 053408 (2014).
[40] E. Torrontegui, S. Martínez-Garaot, and J. G. Muga, Hamiltonian engineering via invariants and dynamical algebra, Phys. Rev. A **89**, 043408 (2014).
[41] S. Martínez-Garaot, A. Ruschhaupt, J. Gillet, Th. Busch, and J. G. Muga, Fast quasiadiabatic dynamics, Phys. Rev. A **92**, 043406 (2015).
[42] C. Jarzynski, Generating shortcuts to adiabaticity in quantum and classical dynamics, Phys. Rev. A **88**, 040101(R) (2013).

[43] S. Deffner, C. Jarzynski, and A. del Campo, Classical and Quantum Shortcuts to Adiabaticity for Scale-Invariant Driving, Phys. Rev. X **4**, 021013 (2014).
[44] A. Patra and C. Jarzynski, Classical and quantum shortcuts to adiabaticity in a tilted piston, J. Phys. Chem. B **121**, 3403 (2017).
[45] M. Okuyama and K. Takahashi, Quantum-classical correspondence of shortcuts to adiabaticity, J. Phys. Soc. Jpn. **86**, 043002 (2017).
[46] X. J. Lu, J. G. Muga, X. Chen, U. G. Poschinger, F. Schmidt-Kaler, and A. Ruschhaupt, Fast shuttling of a trapped ion in the presence of noise, Phys. Rev. A **89**, 063414 (2014).
[47] A. E. Allahverdyan and Th. M. Nieuwenhuizen, Minimal work principle: Proof and counterexamples, Phys. Rev. E **71**, 046107 (2005).
[48] A. E. Allahverdyan and Th. M. Nieuwenhuizen, Minimal-work principle and its limits for classical systems, Phys. Rev. E **75**, 051124 (2007).
[49] M. Robnik and V. G. Romanovski, Exact analysis of adiabatic invariants in the time-dependent harmonic oscillator, J. Phys. A **39**, L35 (2006).
[50] M. Palmero, E Torrontegui, D. Guéry-Odelin, and J. G. Muga, Fast transport of two ions in an anharmonic trap, Phys. Rev. A **88**, 053423 (2013).
[51] M. Palmero, R. Bowler, J. P. Gaebler, D. Leibfried, and J. G. Muga, Fast transport of mixed-species ion chains within a Paul trap, Phys. Rev. A **90**, 053408 (2014).
[52] M. Palmero, S. Martínez-Garaot, J. Alonso, J. P. Home, and J. G. Muga, Fast expansions and compressions of trapped-ion chains, Phys. Rev. A **91**, 053411 (2015).
[53] M. Palmero, S. Martínez-Garaot, U. G. Poschinger, A. Ruschhaupt, and J. G. Muga, Fast separation of two trapped ions, New J. Phys. **17**, 093031 (2015).
[54] X. J. Lu, M. Palmero, A. Ruschhaupt, X. Chen, and J. G. Muga, Optimal transport of two ions under slow spring-constant drifts, Phys. Scr. **90**, 074038 (2015).
[55] M. Palmero, S. Wang, D. Guéry-Odelin, Jr-Shin Li, and J. G. Muga, Shortcuts to adiabaticity for an ion in a rotating radially-tight trap, New J. Phys. **18**, 043014 (2016).
[56] M. Palmero, S. Martínez-Garaot, D. Leibfried, D. J. Wineland, and J. G. Muga, Fast phase gates with trapped ions, Phys. Rev. A **95**, 022328 (2017).
[57] I. Lizuain, M. Palmero, and J. G. Muga, Dynamical normal modes for time-dependent Hamiltonians in two dimensions, Phys. Rev. A **95**, 022130 (2017).
[58] H. R. Lewis and P. G. L. Leach, A direct approach to finding exact invariants for one-dimensional time-dependent classical Hamiltonians, J. Math. Phys. (N.Y.) **23**, 2371 (1982).
[59] A. Tobalina, M. Palmero, S. Martínez-Garaot, and J. G. Muga, Fast atom transport and launching in a nonrigid trap, Sci. Rep. **7**, 5753 (2017).
[60] X. Chen, E. Torrontegui, D. Stefanatos, J. S. Li, and J. G. Muga, Optimal trajectories for efficient atomic transport without final excitation, Phys. Rev. A **84**, 043415 (2011).
[61] E. Torrontegui, X. Chen, M. Modugno, S. Schmidt, A. Ruschhaupt, and J. G. Muga, Fast transport of Bose-Einstein condensates, New J. Phys. **14**, 013031 (2012).
[62] D. Stefanatos, J. Ruths, and J. S. Li, Frictionless atom cooling in harmonic traps: A time-optimal approach, Phys. Rev. A **82**, 063422 (2010).
[63] Q. Zhang, J. G. Muga, D. Guéry-Odelin, and X. Chen, Optimal shortcuts for atomic transport in anharmonic traps, J. Phys. B **49**, 125503 (2016).
[64] E. Torrontegui, I. Lizuain, S. González-Resines, A. Tobalina, A. Ruschhaupt, R. Kosloff, and J. G. Muga, Energy consumption for shortcuts to adiabaticity, Phys. Rev. A **96**, 022133 (2017).
[65] N. Sun, Y. Fang, X. Zhang, and Y. Yuan, Transportation task-oriented trajectory planning for underactuated overhead cranes using geometric analysis, IET Control Theory Appl. **6**, 1410 (2012).
[66] A. Couvert, T. Kawalec, G. Reinaudi, and D. Guéry-Odelin, Optimal transport of ultracold atoms in the non-adiabatic regime, Europhys. Lett. **83**, 13001 (2008).
[67] A. Zenesini, H. Lignier, D. Ciampini, O. Morsch, and E. Arimondo, Coherent Control of Dressed Matter Waves, Phys. Rev. Lett. **102**, 100403 (2009).
[68] H. Goldstein, C. Poole, and J. Safko, *Classical Mechanics*, 3rd ed. (Addison-Wesley, Reading, MA, 2002).
[69] See http://functions.wolfram.com/Constants/E/.
[70] I. S. Gradshteyn and I. M. Ryzhik, *Table of Integrals, Series, and Products*, 7th ed. (Academic Press, Amsterdam, 2007).
[71] *Handbook of Mathematical Functions*, edited by M. Abramowitz and I. A. Stegun (Dover, New York, 1972), Chap. 17.